Journal of Chromatography, 536 (1991) 289–301
Elsevier Science Publishers B.V., Amsterdam

CHROMSYMP. 2002

Refractive index gradient detection of biopolymers separated by high-temperature liquid chromatography

CURTISS N. RENN and ROBERT E. SYNOVEC*
Center for Process Analytical Chemistry, Department of Chemistry, BG-10, University of Washington, Seattle, WA 98195 (U.S.A.)

ABSTRACT

A refractive index gradient (RIG) detector has been successfully applied in both mobile phase gradient (MPG) and thermal gradient (TG) microbore liquid chromatography (μLC). The RIG detector is based upon probing the radial RIG of the material passing through a small-volume *z*-configuration flow cell with a 390-μm internal radius. The optimum RIG sensitivity was at a position of 225 μm offset parallel to the flow cell center axis. This optimum position was probed by a 200-μm diameter collimated laser beam produced by fiber optic techniques. The performance of MPG-μLC and TG-μLC with RIG detection was evaluated using mixtures of *n*-alkanes and 1,2-diacylphosphatidylcholines (a class of phospholipid biopolymers). Baseline drift for the gradient separations was found to be quite small, in contrast to the performance one would obtain using conventional RI detection. Furthermore, the detection limit for the integrated RIG signal was routinely $2 \cdot 10^{-8}$ RI units (3 × baseline root mean square noise). The technique of TG-μLC with RIG detection was found to dramatically reduce the analysis time for the biopolymer separation, while providing detection limits below 100 ng injected phospholipid.

INTRODUCTION

High-temperature–high-performance liquid chromatography (HT-HPLC) is gaining interest as a useful technique for rapidly separating large molecules [1]. The rapid analysis of complex biopolymer samples by HPLC also requires a suitable detector. The analytical challenge is in developing new techniques and instrumentation to meet the need of rapid and confident quantitative analysis in the biotechnology field. While isocratic separations are straightforward, the need to optimize the information content per unit time necessitates the application of gradient elution HPLC [2]. The traditional approach in HPLC employs a mobile phase gradient (MPG), minimally a time-dependent mixing of two solvents of differing elution strength. The need for both rapid separation and rapid recovery to initial mobile phase conditions in the column may make thermal gradient (TG) elution in LC an useful alternative to the conventional MPG, where temperature instead of mobile phase composition is changed with time [3]. One of the experimental considerations in TG elution is the requirement for rapid thermal "equilibration" of the column as

0021-9673/91/$03.50

a function of temperature. Microbore columns meet this requirement, thus the technique of thermal gradient microbore liquid chromatography (TG-μLC) should be well suited for rapid process analysis of biopolymers.

Detection of biopolymers and related species separated by HPLC has been difficult, since many analytes of interest do not exhibit an useful chromophore, inhibiting direct absorbance and fluorescence detection [4]. While derivatization with a chromophore is possible, the approach is often time consuming and compatibility with gradient elution is seldom developed. The conventional refractive index (RI) detector is not compatible with either MPG-μLC or TG-μLC primarily due to two factors. First, large baseline drifts result from the detection mechanism, *i.e.*, the bulk RI of the effluent is measured [5]. Second, the need to minimize band broadening prohibits the application of sequential differential RI detection [6,7]. Nonetheless, the universal nature of the RI detector response is appealing. To solve many of these deficiencies, a mass detector based upon light scattering from non-volatile solute particles following preferential evaporation of the mobile phase (solvent) has been developed [8,9]. The mass detector works quite well for MPG-μLC separations for several biopolymer samples, but is hampered by the requirement that the mobile phase be volatile to function properly, thus mobile phase selection is generally limited to volatile organics, precluding the application of popular aqueous buffers. Indirect detection also provides universal detection of analytes with absolute quantitation [10,11]. While indirect detection may also prove useful for gradient elution μLC, demonstration has not been reported and baseline stability may be a problem. All of the previously mentioned detectors have not been hyphenated to TG-μLC, although work in this direction might prove fruitful once the technical problems have been addressed [3], as is the focus of the work reported here.

A sensitive universal detector that is readily amenable to both MPG-μLC and TG-μLC, and can be applied in conjunction with popular aqueous buffers, would be quite useful for many biopolymer separations. The refractive index gradient (RIG) detector, which is not to be confused with the conventional RI detector, meets these criteria. While the RIG detector development has a complicated past, the first report was made by Betteridge *et al.* [12] where the authors provided a concise, yet qualitative, description of the detection mechanism. Later, Pawliszyn [13–15] provided a more detailed description of a RIG detector for HPLC, where the RIG along the direction of the effluent flow (axial) is probed. The RIG detector that we have been developing [16–18] involves carefully probing the radial concentration gradient [12,19], not the axial concentration gradient, resulting in a considerable improvement in detection sensitivity, and thus ease in detector design and application. Since the detection mechanism results in probing the RIG in the flow cell, there is a sensitivity "preference" for spatially sharp concentration profiles, such as chromatographic peak, while slowly changing concentration profiles, such as a MPG or TG contribute a minimal extent to the detected signal. While the merits of the RIG detector for HPLC were clearly outlined in the work of Pawliszyn [13], experimental evidence of a RIG detector performing in gradient elution HPLC has not been published.

In this paper we report the first use of RIG detection for MPG-μLC and TG-μLC. A test mixture of *n*-alkanes is separated by reversed-phase (RP) μLC in order to evaluate the detector performance under isocratic, binary MPG, and TG separation conditions. The relationship between the MPG program and the RIG-detected

baseline is examined with guidelines reported, and compared in principle to the baseline one would observe with a conventional RI detector. Results will demonstrate that indeed the technique of TG-μLC with RIG detection is simple, yet effective, in providing optimized resolving power with sensitive, universal detection. Thus, TG-μLC was applied to a RP separation of a test mixture of high molecular weight 1,2-diacylphosphatidylcholines (DAPCs), a class of phospholipids known to be difficult to analyze by HPLC due to solubility difficulties, and by gas chromatography due to the required, tedious sample derivatization and pretreatment procedures [4,9,20]. The technique of RP-TG-μLC is shown to not require the ion pairing reagent choline chloride, commonly added to improve elution behavior [4]. Essentially, the TG technique is shown to dramatically improve the separation through "programmed solubility" of the DAPCs. Further, the RIG detector is shown to perform admirably with the TG-μLC separation of DAPCs. Other details that are addressed include RIG detector design in the context of minimizing band broadening, optimization of the sensitivity, and the detection limit for the device.

EXPERIMENTAL

Refractive index gradient detector

A schematic of the apparatus used in this work is shown in Fig. 1a. The 633-nm, 5-mW continuous wave (cw) output from a HeNe laser (1305 P; Uniphase, Sunnyvale, CA, U.S.A.) was focused by a 20× microscope objective (M-20×; Newport Corp., Fountain Valley, CA, U.S.A.) onto an optical fiber (6 μm core, 125 μm clad, 175 μm

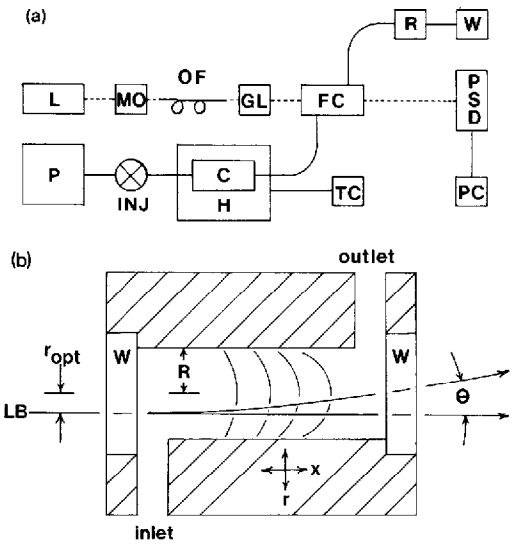

Fig. 1: (a) Apparatus for both MPG-μLC and TG-μLC with RIG detection. L = Laser; MO = microscope objective; OF = optical fiber; GL = GRIN-lens; FC = flow cell; PSD = position-sensitive detector; PC = personal computer; P = MPG syringe pump system; INJ = injection valve; H = heater; C = column; TC = temperature controller; R = pressure restrictor; W = waste. (b) z-Configuration flow cell. LB = Laser beam; r_{opt} = optimum radial position of probe beam; W = quartz window; R = radius of flow cell; θ = angular deflection of probe beam; r = radial axis of flow cell; x = length axis of flow cell.

jacket) that was designed for single-mode operation at 633 nm (SM 6/125 Al coated; Fujikura, Tokyo, Japan). A collimated probe beam was produced by interfacing the optical fiber output to a graded refractive index (GRIN) lens that was quarter pitch at 633 nm (NSG America, Somerset, NJ, U.S.A.). The optical fiber and GRIN-lens combination was chosen to obtain a small-diameter, collimated beam to selectively probe the most sensitive radial position for RIG detection in the flow cell. Careful measurement of the beam intensity profile indicated that the probe beam full angle divergence was 3.5 mrad, with an initial diameter of 110 μm, defined as 95% of the beam intensity, at the GRIN-lens output face. The probe beam was directed through a z-configuration flow cell (made in-house) mounted to a high precision x–y–z translational stage (460-XYZ Newport Corp.) with a 2 cm distance separating the flow cell and the GRIN-lens. The flow cell was constructed of polyetheretherketone (PEEK) with a 6 mm optical pathlength and a 780-μm internal diameter, comprising a total internal volume of 2.9 μl, with liquid flow entering and exiting in the vertical plane. The probe beam was aligned at the optimum radial position for maximum RIG detection sensitivity as shown in Fig. 1b, and on the horizontal axis to avoid possible flow perturbations at the flow inlet and outlet positions. The probe beam was at an average diameter of 200 μm in the flow cell so we could selectively probe the most sensitive radial position. For the flow cell used in this work, the optimal radial position, r_{opt}, was 225 μm. The measured length variance of a chromatographic peak (s_x^2) in the context of the flow cell can be calculated by the sum of the length variance of the peak before detection (s_v^2) plus the length variance contribution of the flow cell by

$$s_x^2 = \left(\frac{s_v}{\pi R^2}\right)^2 + \frac{R^2 L v}{24 D_m} \tag{1}$$

where R is the radius of the flow cell, L the length of flow cell, v the linear flow velocity in the flow cell, and D_m the diffusion coefficient of the analyte of interest. Given a typical μLC peak width of 40 μl at the base, standard deviation (s) = 10 μl, and given R = 390 μm, v = 3.48 mm/s in the flow cell (for a typical volumetric flow-rate of 100 μl/min), and $D_m = 5 \cdot 10^{-3}$ mm^2/s, the length variance of the peak is 438 mm^2 and 465 mm^2 before and after detection, respectively, corresponding to only 3% additional band broadening due to the flow cell. Using pure acetonitrile as the solvent, the calculated Reynolds number for the flow cell is 2.6, well within the Poiseuille flow range required to obtain consistent detector performance. Quartz windows were placed over the ends of the flow cell and sealed with polymer O-rings to provide an optical window and high pressure flow cell. After the collimated probe beam passed through the flow cell, it was incident on a position-sensitive detector (S1352; Hamamatsu, Hamamatsu, Japan) with dimensions of 33 mm × 2.5 mm, placed a distance of 83 cm from the flow cell.

Microbore HPLC system

For the MPG separation, the solvent delivery system consisted of two syringe pumps (μLC-500; ISCO, Lincoln, NE, U.S.A.) to deliver the chromatographic mobile phase to a microscale mixer (Upchurch, Oak Harbor, WA, U.S.A.) with an internal volume of 3.2 μl. A 152-cm coiled length of 1/16 in. O.D. × 0.020 in. I.D. PEEK tubing (Upchurch) followed the mixer to provide additional mixing for use with the MPG.

The injection valve (7520; Rheodyne, Cotati, CA, U.S.A.) fitted with a 1-μl injection disk. A μLC column was connected to the microbore injection valve via a 5-cm length of 1/16 in. O.D. × 0.005 in. I.D. PEEK tubing (Upchurch). A 250 mm × 1 mm column with 5 μm, silica based octyl packing (Deltabond; Keystone, Bellefonte, PA, U.S.A.) was used with the separations of *n*-alkanes, and a 200 mm × 1 mm column packed with PRP 10-μm resin (Suprex, Pittsburgh, PA, U.S.A.) was used with the TG-μLC separation of phosphatidylcholines. The columns were placed on a heating strip (SS2181; Wellman, Shelbyville, IN, U.S.A.) with thermal contact to the heater accomplished via thermal joint compound and the temperature controlled by a FIAtron controller (TC-55; FIAtron, Oconomowoc, WI, U.S.A.) used only for the TG-μLC separations. The effluent from the column was delivered to the flow cell via a short length of low-dispersion tubing. After exiting the flow cell, the column effluent passed through a pressure restrictor (Upchurch) rated at 250 p.s.i.g. and subsequently to waste.

Chromatographic conditions and reagents

The MPG-μLC separation of *n*-alkanes consisted of a binary mixture with a composition by %(v/v) of A (acetonitrile–diethyl ether, 90:10) and B (water–acetonitrile–diethyl ether, 50:45:5) at a constant flow-rate of 100 μl/min, with the A–B ratio given in the figure captions. In all cases, the MPG was linear from A–B (80:20) to 100% A over the time specified in the figure captions. The TG-μLC separation of *n*-alkanes consisted of A–B (70:30) at a flow-rate of 100 μl/min with the temperature profiles given in the respective figure. The isothermal (25°C) and TG-μLC separation of DAPCs consisted of 100% methanol at 50 μl/min. All mobile phases consisted of HPLC-grade solvents (Baker Analyzed; J. T. Baker, Phillipsburg, NJ, U.S.A.). Reagent-grade DAPCs and *n*-alkanes (Sigma, St. Louis, MO, U.S.A.) were used as test mixtures.

Data collection and analysis

Chromatographic data were collected via laboratory interface (DASH-16; Metra Byte, Taunton, MA, U.S.A.), which facilitated the analog-to-digital (A/D) conversion of the signal from the position-sensitive detector and subsequently stored on a personal computer (IBM-XT, Armonk, NY, U.S.A.) for further data processing. The data collected for the alkane separations were not at an optimal signal-to-noise ratio (S/N) due to a noisy data acquisition input; however, the absolute angular deflection is accurate and therefore the operation of the RIG detector can be objectively investigated with TG- and MPG-μLC separations. Subsequent analysis of DAPCs was optimized for S/N considerations with detection limits expressed as three times the standard deviation of the baseline noise.

RESULTS AND DISCUSSION

Mobile phase gradient and isocratic separations

The use of the RIG detector with μLC will be illustrated by working through isocratic separations of *n*-alkanes, with subsequent optimization by MPG-μLC. An isocratic RP-μLC separation of *n*-alkanes using a relatively strong mobile phase is shown in Fig. 2a where the injection disturbance at 2 min marked the elution time of an

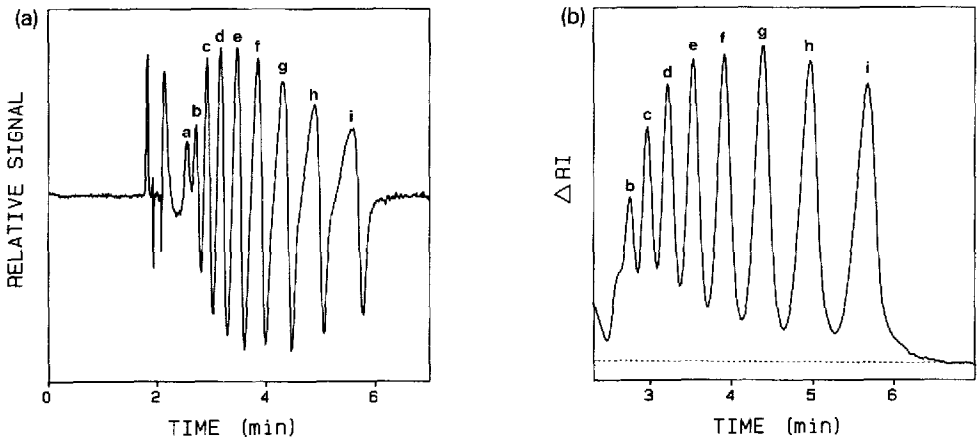

Fig. 2. (a) Microbore isocratic separation of *n*-alkanes at room temperature (25°C) with RIG detection. Peaks: a = *n*-pentane; b = *n*-hexane; c = *n*-heptane; d = *n*-octane; e = *n*-nonane; f = *n*-decane; g = *n*-undecane; h = *n*-dodecane; i = *n*-tridecane. Mobile phase, 100% A (as defined in Experimental section) at 100 μl/min. (b) Running total integration of the chromatogram shown in (a).

unretained analyte. The analytical signal consisted of a positive and negative going peak as previously described [12–19], corresponding to the derivative of the RI profile eluted from the μLC column. This unconventional signal can be cast into a more familiar form by performing the running total integration (RTI) [14,21,22] to obtain the RI profile eluting from the μLC column as shown in Fig. 2b. Baseline resolution is given by the dashed line on the bottom of the figure, indicating incomplete resolution for all of the analytes with *n*-pentane forming a shoulder on the side of *n*-hexane, furthermore, complicated by *n*-pentane falling on the tail of the injection disturbance, precluding confident quantitation. The RTI algorithm was successfully applied to all chromatograms, however for subsequent chromatograms only the RIG signal will be shown for brevity.

A simple solution to the lack of chromatographic resolution is to decrease the strength of the mobile phase, thus increasing the water content of the mobile phase resulted in the chromatogram shown in Fig. 3. Inspection of the integrated chromatogram from Fig. 3, not shown for brevity, indicated baseline resolution for all the analytes, *n*-pentane through *n*-tridecane. The limitation of this approach to increase chromatographic resolution is long analysis time, nearly 20 min for the same analyte mixture, and excessive peak broadening of the later eluting peaks, resulting in inferior detectability.

An alternative solution to increasing chromatographic resolution is to perform a MPG to dynamically change the retention behavior of later eluting analytes, allowing the optimization of resolution throughout the entire chromatogram. The MPG should provide a shorter analysis time while not sacrificing resolution for early eluting analytes and optimizing detection for later eluting analytes [2]. Traditionally, MPG-μLC separation capability was not compatible with RI detection since the measured analytical signal was proportional to the bulk RI of the column effluent [5]. It was therefore prohibitively difficult to keep the signal for a conventional RI detector on scale for a typical MPG separation of interest. For RP-μLC separations, a large

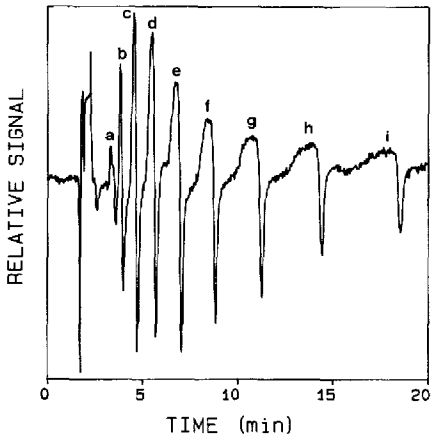

Fig. 3. Isocratic separation of *n*-alkanes at room temperature (25°C) with RIG detection. Mobile phase, A–B (80:20, v/v) (as defined in Experimental section) at 100 μl/min. Peaks as in Fig. 2a.

change in solvent strength would be to start with 100% water and finish with 100% methanol, comprising a RI change of 0.0046, much too large of a RI change to be useful for a conventional RI detector. Furthermore, the problem of poor sensitivity and limited dynamic range for conventional RI detection cannot be solved by injecting a high concentration, since overloading of the column will occur. Thus, the inherent sensitivity and limited dynamic detection range of conventional RI detection precludes the application of a MPG in μLC.

The first published report of a MPG-μLC separation with RIG detection is presented in Fig. 4a with the entire analysis time under 10 min for baseline resolution of all *n*-alkanes. The MPG started with the same composition as the chromatogram in Fig. 3 to obtain baseline resolution of the early eluting analytes with a linear change of the mobile phase composition to the stronger eluent used for Fig. 2 to optimize resolution of later eluting analytes. Collection of the MPG baseline (Fig. 4b) and MPG-μLC separation (Fig. 4a) on a computer allowed further data analysis by subtraction of the MPG baseline from the MPG separation to remove the baseline drift as shown in Fig. 4c. This simple data manipulation technique allows baseline correction for subsequent integration and further inspection of the separation.

A more critical evaluation of the baseline signal obtained in MPG-μLC as shown in Fig. 4b is warranted. Integration of Fig. 4b yields the total RI change for the mobile phase gradient as shown by Fig. 5, trace B. Additionally, 2.5- and 10-min gradients were also collected and integrated as shown by traces A and C, respectively. Integration to essentially the same RI value indicates that the RI signal is conserved and independent of the steepness of the gradient formation, providing evidence that the RIG detector is functioning properly.

From Fig. 5, the RI changed by $6 \cdot 10^{-4}$ RI over the 5-min linear MPG, shown in Fig. 4B, corresponding to an angular deflection of the baseline by only 600 μrad as given in Table I. The RIG detector signal was found to be well-behaved to 10 mrad, indicating a maximum useable eluent range of 0.01 RI for a 5 minute gradient. As

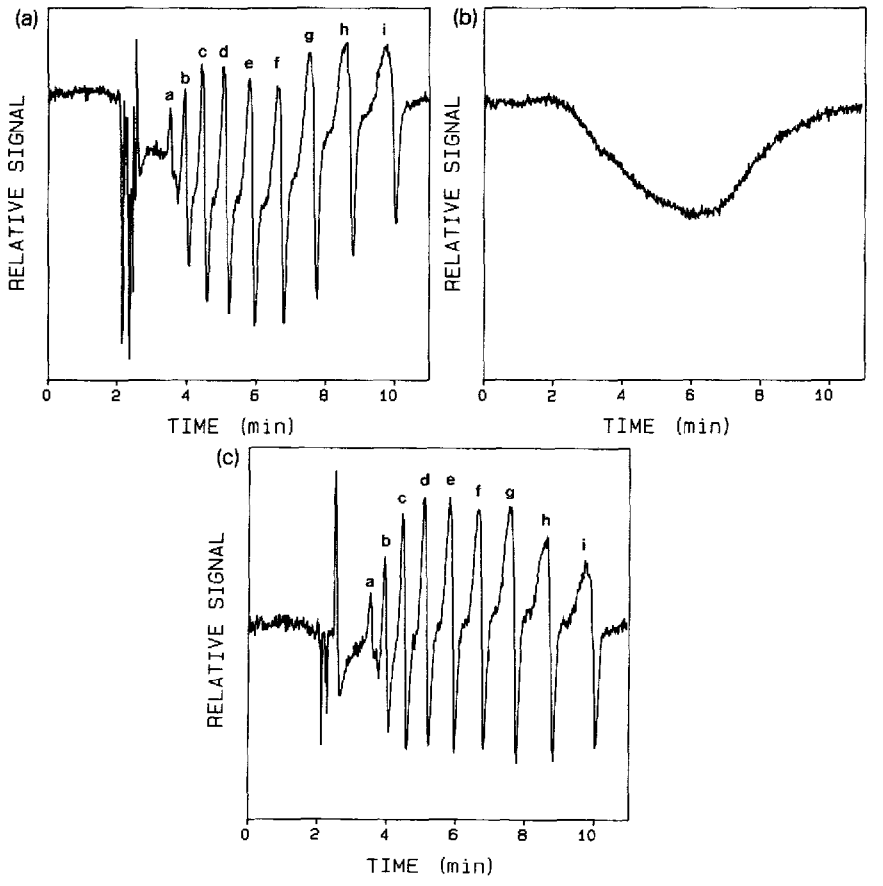

Fig. 4. (a) MPG-μLC separation of *n*-alkanes at room temperature (25°C) with RIG detection. Linear MPG from A–B (80:20) to 100% A (as defined in Experimental section) over 5-min interval at 100 μl/min. Peaks as in Fig. 2a. (b) Baseline for MPG-μLC with RIG detection. No sample injected. Chromatographic conditions as in (a). (c) Baseline corrected MPG-μLC separation of *n*-alkanes with RIG detection [(a) minus (b)]. Peaks as in Fig. 2a.

indicated by Table I, a longer gradient delivery time results in a reduced baseline response, thereby increasing the useful RI range that can be accommodated. For instance, a 10-min MPG program would result in a maximum allowable baseline angular deflection of 10 mrad if the absolute RI change is 0.02 RI, well beyond the RI change resulting from a 100% water to 100% methanol MPG (0.0046 RI change). Compared to conventional RI detection there is a considerable increase in useful dynamic range for mobile phase composition change using RIG detection.

Thermal gradient separations of n-alkanes

A more attractive solution to reduce analysis time while optimizing the column resolving power is to perform a thermal gradient (TG-μLC) separation. A potential benefit of TG-μLC is reproducible temperature control and thus reproducible

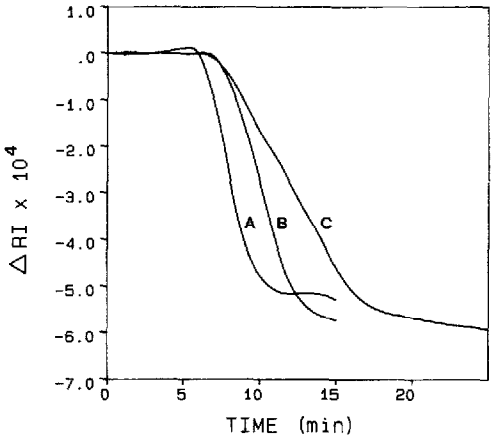

Fig. 5. Integrated RIG detected baseline drift from MPGs. A = 2.5-min gradient; B = 5.0-min gradient; C = 10.0-min gradient. Linear MPG from A–B (80:20) to 100% A (as defined in Experimental section) at 100 μl/min over specified time intervals.

separation conditions, in contrast to the difficulties often encountered with reproducible MPG formation. Another distinct advantage of TG-μLC is the simplicity of the instrumentation, requiring only one pump, heater and temperature controller, in contrast to MPG-μLC requiring two syringe pumps, microscale mixer and gradient pump controller. To perform sensitive detection via conventional RI detection, commonly requires thermostating the column and detector in an oven by ± 0.01 C, preventing the use of conventional RI detection with TG-μLC.

The first report of a TG-μLC separation with RI-based detection is shown in Fig. 6 for the same *n*-alkane mixture used in the isocratic and MPG-μLC separations. Comparing the analysis time in Fig. 4a and Fig. 6 clearly indicates that TG-μLC is an effective alternative to MPG-μLC. The temperature profile of the TG program is given by the dashed line in Fig. 6. Even though no attempt was made to thermostat the flow cell to the temperature of the incoming column effluent, the baseline drift of 500 μrad was less than observed for the MPG-μLC separation for a similar analysis time. Future improvements to the instrument will include placement of the flow cell in the same temperature environment as the column, eliminating any problems due to non-equilibrium temperature conditions between the flow cell and the column effluent. The

TABLE I

BASELINE DRIFT WITH RIG DETECTION AT VARIOUS MPG RATES

Gradient conditions given in Experimental section.

Gradient (min)	Baseline drift[a] (μrad)
2.5	900
5.0	600
10	280

[a] Drift defined by RIG maximum to minimum baseline signal for MPG.

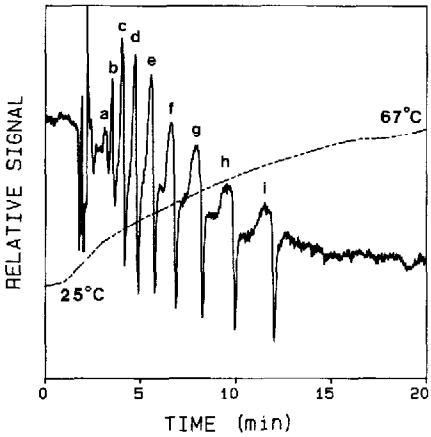

Fig. 6. TG-μLC separation of *n*-alkanes with RIG detection. Temperature program given by dashed line. Mobile phase, A–B (70:30) (as defined in Experimental section) at 100 μl/min. Peaks as in Fig. 2a.

technique of subtracting the TG-μLC baseline drift from the TG-μLC separation can be used to correct the data for baseline drift, as described for the MPG-μLC separation.

Bioseparations

A resin-based μLC column was chosen for the separation of DAPCs to allow separation of DAPCs without the use of modifiers or buffers typically used with reversed-phase silica-based columns [4]. Furthermore difficulties associated with dissolution of silica column packing material were eliminated by using a polymer-based column. A generic structure of a DAPC is shown in Fig. 7, with the largest DAPC used in this study approaching a molecular weight of 800 g/mole. Four DAPCs, as defined by Fig. 7 and Table II, were used as a test mixture. An isothermal separation of DAPCs is shown in Fig. 8, clearly indicating the need for gradient separation capability, evident by near baseline resolution at the beginning of the separation with excessive resolution and long analysis time for the complete separation [4,9,20] with the last peak severely broadened. The detection limit for DLPC was 36 ng injected mass, with an angular detection limit of 2 μrad, and a RI detection limit of $2 \cdot 10^{-8}$ RI. In principle, one could utilize a PSD with a better angular sensitivity to achieve a better

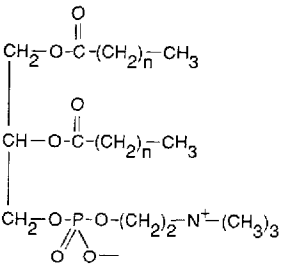

Fig. 7. General structure of 1,2-diacylphosphatidylcholine. See Table II for definition of species analyzed.

TABLE II

IDENTIFICATION OF 1,2-DIACYLPHOSPHATIDYLCHOLINES (DAPCs)

These four DAPCs comprise a mixture defined according to the value of n, as applied in Fig. 7.

n	Common name[a]	Abbreviation
10	Dilauryl	DLPC
12	Dimyristyl	DMPC
14	Dipalmityl	DPPC
16	Distearyl	DSPC

[a] Fatty acid chain = $n+2$, (diacyl-).

RI and mass detection limit, however, in practice the angular detection limit is not limited by the sensitivity of the position-sensitive detector but rather limited by minor flow perturbations in the flow cell.

Previous work with the RIG detector [16] has shown RI detectability to be inversely proportional to the peak width and analyte detectability to be inversely proportional to the peak variance and therefore an more efficient separation is a viable solution to yield better detectability. The polymer column used for this work was chosen for potential use with low-pressure LC instrumentation and therefore efficiency was traded for low column back pressure. The pressure for the isothermal separation of DAPCs was only 600 p.s.i. including the 250-p.s.i. pressure restrictor, thereby allowing a wide variety of solvent delivery and injection systems compatible with the column and RIG detector. Alternatively, where detection limits are a major concern, selection of a higher efficiency column yielding peak widths of 25 μl at the base instead of 100 μl would result in mass detection limits 16 times lower, or 2 ng injected DLPC.

Rapid analysis of the same DAPC mixture shown in Fig. 8 by TG-μLC with RIG detection is shown in Fig. 9 with the analysis time reduced by a factor of about 2.5 from

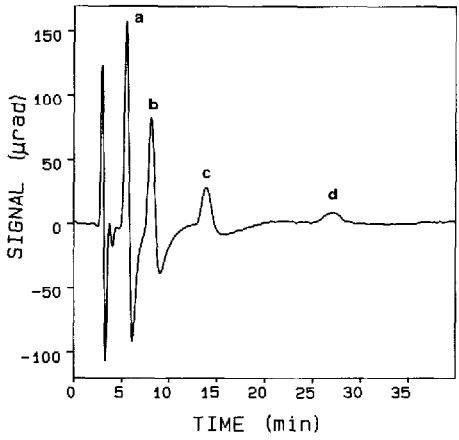

Fig. 8. Isothermal (25°C) separation of DAPCs defined in Table II and Fig. 7. Peaks: a = DLPC; b = DMPC; c = DPPC; d = DSPC. Mobile phase, 100% methanol at 50 μl/min. Injected mass, 8 μg of each DAPC.

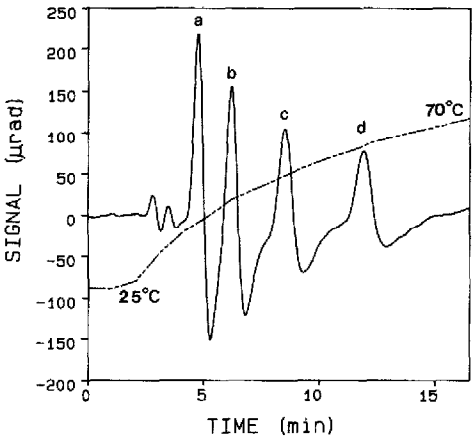

Fig. 9. TG-μLC separation of the same mixture of DAPCs shown in Fig. 8. Temperature profile given by dashed line. Mobile phase, 100% methanol at 50 μl/min. Peaks as in Fig. 8.

the room temperature separation. The capacity factor for DSPC changed from 9.0 to 3.2 from the isothermal separation to the TG-μLC separation. Furthermore, detectability of DSPC for the TG separation relative to the isothermal separation is better by a factor of 14 due to a reduction in peak width. The decreased analysis time or increased solvent strength of the TG separation also indicates the capability to elute larger DAPCs normally present in biological samples without loss of resolution for earlier eluting DAPCs. Inspection of Fig. 9 also indicates the baseline drift to be less than 10 μrad, clearly an improvement over the TG-μLC separation of *n*-alkanes (Fig. 6), with a baseline drift of 500 μrad. The primary experimental difference between the DAPC and *n*-alkane separation was the flow-rate of the eluent, indicating a strong flow-rate dependence of non-equilibrium temperature conditions manifested as baseline drift for TG-μLC with RIG detection. This apparent advantage requires further investigation. In general, the technique of TG-μLC with RIG detection appears to be very promising for routine analysis of biopolymers where rapid characterization and confident quantitation is required.

ACKNOWLEDGEMENT

We thank the NSF Center for Process Analytical Chemistry for support of this work (Project Number 89-5).

REFERENCES

1 F. D. Antia and Cs. Horváth, *J. Chromatogr.*, 435 (1988) 1.
2 B. L. Karger, L. R. Snyder and Cs. Horváth, *An Introduction to Separation Science*, Wiley, New York, 1973, p. 161.
3 W. R. Biggs and J. C. Fetzer, *Anal. Chem.*, 61 (1989) 236.
4 A. D. Postle, *J. Chromatogr.*, 415 (1987) 241.
5 M. Munk, in T. Vickers (Editor), *Liquid Chromatographic Detectors*, Marcel Dekker, New York, 1983.

6 S. Banerjee and E. J. Pack, Jr., *Anal. Chem.*, 54 (1982) 324.
7 S. D. Woodruff and E. S. Yeung, *J. Chromatogr.*, 260 (1983) 363.
8 A. S. Stolyhwo, H. Colin and G. Guiochon, *Anal. Chem.*, 57 (1985) 1342.
9 N. Sotirhos, C. Thorngren and B. Herslof, *J. Chromatogr.*, 331 (1985) 313.
10 H. Small and T. E. Miller, *Anal. Chem.*, 54 (1982) 462.
11 D. R. Bobbit and E. S. Yeung, *Anal. Chem.*, 56 (1984) 1577.
12 D. Betteridge, E. L. Dagless, B. Fields and N. F. Graves, *Analyst (London)*, 103 (1978) 897.
13 J. Pawliszyn, *Anal. Chem.*, 58 (1986) 243.
14 J. Pawliszyn, *Anal. Chem.*, 58 (1986) 2307.
15 J. Pawliszyn, *Anal. Chem.*, 60 (1988) 2796.
16 D. O. Hancock and R. E. Synovec, *Anal. Chem.*, 60 (1988) 1915.
17 D. O. Hancock and R. E. Synovec, *Anal. Chem.*, 60 (1988) 2812.
18 D. O. Hancock and R. E. Synovec, *J. Chromatogr.*, 464 (1989) 83.
19 C. E. Evans and V. L. McGuffin, *J. Chromatogr.*, 459 (1988) 119.
20 E. W. Hammond, *Trends Anal. Chem.*, 8 (1989) 308.
21 R. E. Synovec and E. S. Yeung, *Anal. Chem.*, 57 (1985) 2162.
22 R. E. Synovec and E. S. Yeung, *Anal. Chem.*, 58 (1986) 2093.